Terrestrial Measurements of Diffusivities in Refractory Melts by Pulsed Melting of Thin Films

Proceedings of the 2000 Microgravity Materials Science Conference (National Aeronautics and Space Administration, Washington, DC, 2000)

TERRESTRIAL MEASUREMENTS OF DIFFUSIVITIES IN REFRACTORY MELTS BY PULSED MELTING OF THIN FILMS

Paul G. Sanders[1], Michael J. Aziz[1*]

[1] Division of Engineering and Applied Sciences, Harvard University, Cambridge MA

Abstract

Laterally homogeneous pulsed melting of thin films is being investigated as a way to eliminate convection and thereby determine diffusivities in refractory melts under terrestrial conditions, providing comparison data for microgravity measurements. The silicon liquid self-diffusivity was determined by pulsed laser melting of $^{30}Si^{+}$ ion implanted silicon-on-insulator thin films. The broadening of nearly Gaussian solute concentration-depth profiles was determined ex situ using Secondary Ion Mass Spectrometry. Melt depth versus time and total melt duration were monitored by time-resolved lateral electrical conductance and optical reflectance measurements. One-dimensional diffusion simulations were utilized to match the final $^{30}Si^{+}$ experimental concentration spatial profile given the initial concentration profile and the temporal melt-depth profile. The silicon liquid self-diffusivity at the melting point is $(4.0 \pm 0.5) \times 10^{-4}$ cm^2/s. Calculations of buoyancy and Marangoni convection indicate that convective contamination is unlikely.

Introduction

Atomic transport properties of refractory melts such as Si and Ti are important from both a technological and fundamental perspective. We are studying both in the laboratory; here we focus on our results for liquid Si. The ubiquitous use of silicon in the semiconductor industry requires many processing steps, some of which involve liquid phase transport, including Czochralski and float-zone crystal growth, as well as pulsed laser-induced thin film crystallization[1,2]. More accurate knowledge of the liquid diffusivity may therefore help in process modeling and control. From a fundamental standpoint, atomistic simulations of silicon systems are common, but there is a paucity of liquid-phase experimental data, the comparison to which provides a critical test of interaction Hamiltonians and methodology. There are currently many reports of the simulated liquid self diffusivity which are compared only to experimental solute diffusivities due to the absence of an experimental value for the self diffusivity.

Liquid diffusivity is a particularly challenging property to measure accurately. Two potentially serious problems associated with liquid diffusivity measurements are convective contamination and container wall interactions[3]. The elevated melting point (T_m) and high reactivity of Si exacerbate both of these problems. Convective contamination generally occurs when there is a temperature gradient in the liquid, creating instabilities that lead to the formation of convective currents. The likelihood of convection is increased at high temperatures and extended times.

Although it is exceedingly difficult to eliminate completely convective contamination in terrestrial diffusion measurements, these effects are reduced by fine capillaries that make it difficult to establish convection currents. Although container wall interactions have been ruled out in some diffusion experiments with low T_m materials[4], the general concern that fine capillaries can introduce problems with wall interactions is appropriate when working with reactive materials at high temperatures.

Liquid diffusivity measurements made by pulsed laser melting can minimize some of the difficulties in making accurate diffusion measurements. The thin film geometry and short melt duration make it virtually impossible to establish convection currents. The planar geometry permits accurate measurement of the sub-micron diffusion distances resulting from the short melt duration, using techniques such as Rutherford backscattering spectrometry or secondary ion mass spectrometry (SIMS). Because the melted materials are contained by a solid of the same composition, container wall interactions are minimized. Difficulties inherent in this method are the accurate measurement of the melt-depth vs. time profile and the liquid temperature. The agreement between time-resolved reflectivity measurements (TRR), SIMS concentration-depth profiles, and heat-flow simulations can minimize uncertainties in both of these quantities.

Although there have been no reports of self diffusion in liquid Si, there have been measurements of solute diffusivity in silicon and also molecular dynamics simulations of self-diffusion. The chemical similarity of silicon and germanium should lead to comparable magnitudes for silicon liquid self-diffusivity and germanium solute diffusivity in liquid Si. A Ge solute diffusivity of 2.5×10^{-4} cm^2/s has been determined in studies of solute partitioning[5] during rapid solidification, in which the solute liquid diffusivity is a fitting parameter in the analysis. Molecular dynamics simulations yield silicon self-diffusivities at T_m in the range of $0.6 - 2.0 \times 10^{-4}$ cm^2/s (Table I). Simulations using the classical Stillinger-Weber potential have found a weakly activated Arrhenius-type temperature dependence of the silicon liquid self-diffusivity[11,12]. This dependence can be equally well described by a linear temperature dependence over the entire simulated temperature range (1600-1900 K).

Table I. Molecular Dynamics Simulations

Method	Si liquid self-diffusivity (10^{-4} cm^2/s)
ab initio pseudopotentials	1.9 (1800 K)[a], 2.3 (1800 K)[b]
Tight-binding	1.1 (1740 K)[c], 1.3 (1780 K)[d], 1.7 (1780 K)[e]
Stillinger-Weber	0.64 (1700 K)[f], 0.65 (1683 K)[g], 0.69 (1691 K)[h]

a. Ref. 6 b. Ref. 7 c. Ref. 8 d. Ref. 9
e. Ref. 10 f. Ref. 11 g. Ref. 12 h. Ref. 13

Experimental

The silicon-on-insulator (SOI) samples were fabricated by sequential low-pressure chemical vapor deposition (LPCVD) of both SiO_2 and Si films onto (001) Si wafers. Ion implantation of $^{30}Si^+$ at 100 keV to a dose of 4×10^{16} cm^2 produced a $^{30}Si^+$ peak 6 at% above the natural background of 3.1 at% at a depth of 150 nm. The samples were irradiated by a pulsed $XeCl^+$ excimer laser beam (308 nm, 25 ns FWHM; ~50 ns total duration). The specimens were melted from 1 to 5 times using a nominal fluence of 0.75 J/cm^2, which typically produced a melt

duration of 155 ns and a melt depth of 180 nm. The $^{30}Si^{+}$ depth profiles were determined by SIMS. The $^{30}Si^{+}$ concentration calibration was made using the ratio of the $^{30}Si^{+}$:$^{28}Si^{+}$ ion yield.

Data Analysis

The top portion of the silicon film was amorphous after $^{30}Si^{+}$ ion implantation. The initial low-fluence shot resulted in explosive crystallization[14] mediated by a very short-lived melt, yielding a slight change in the $^{30}Si^{+}$ concentration upon crystallization (Fig. 1). This "crystallized" profile was the initial concentration profile used in all diffusion simulations. One-dimensional heat-flow calculations[15,16] using silicon thermophysical properties[17] were used to simulate the laser melt profiles. During resolidification, the TCM melt profiles agreed well with simulated melt profiles calculated for the same laser fluence. The fluences used in the melt profile calculation were selected by matching the melt durations measured by TRR. The simulated fluence was 0.01 to 0.02 J/cm^2 less than the experimental fluence, most likely resulting from variations in the sample surface reflectivity from the literature value.

The simulated silicon melt depth vs. time profile and initial solute concentration-depth profile (after crystallization) were used in solving the one-dimensional diffusion equation[18] to obtain the final solute concentration profile. For each sample, the simulated fluence was varied from 0.74 to 0.76 J/cm^2 and the diffusivity was varied from 2 x 10^{-4} to 6 x 10^{-4} cm^2/s to minimize chi-squared between the final calculated diffusion profile and the final measured $^{30}Si^{+}$ profile. The slight fluence adjustment was needed to match the melt depths observed in the SIMS profiles. To account for the spatial energy variation of the laser beam, reported diffusion profiles were a Gaussian-weighted average of a suite of diffusion profiles calculated at the best-fit fluence ± 3% (the measured spatial variation of the laser beam).

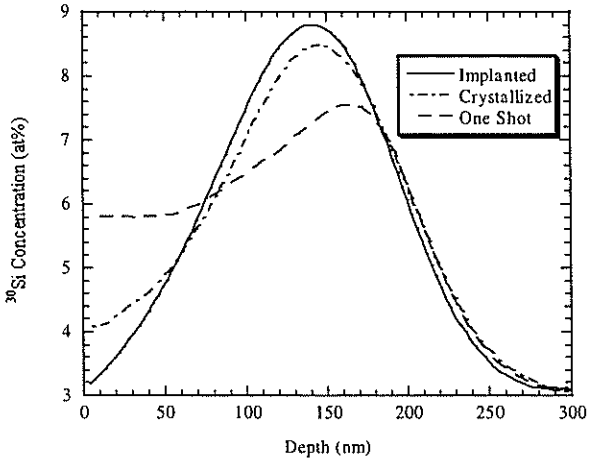

Fig. 1. Concentration depth profiles of $^{30}Si^{+}$ from SIMS, showing as implanted profile and the changes after a low fluence shot (0.30 J/cm^2) for crystallization and a higher fluence shot (0.75 J/cm^2) typical of those used for the diffusion calculations. The crystallized profile was used as the initial condition for the diffusion calculations.

Results and Discussion

The average and standard error of the four measurements reported in Table II for the silicon liquid self-diffusivity at the melting point are (4.0 ± 0.3) x 10^{-4} cm^2/s. Additional uncertainties in the melt profile calculation and SIMS calibration increase the standard error to (4.0 ± 0.5) x 10^{-4} cm^2/s. In Table II, the average experimental melt duration is the average melt duration per shot determined from reflectivity, whereas the average simulated melt duration is the best-fit melt duration used in the diffusion calculations. An indication of the analysis sensitivity can be

obtained from Fig. 2, in which the $^{30}Si^{+}$ SIMS profile for the sample shot 2 times is plotted with diffusion simulations at D = 2, 4, and 6 x 10^{-4} cm^2/s. Clearly 4 x 10^{-4} cm^2/s is the best fit of the three.

Table II. $^{30}Si^{+}$ Liquid Self-Diffusivity Measurements

Number of Shots	Average Melt Duration (Measured) (ns)	Average Melt Duration (Simulated) (ns)	Diffusivity (cm^2/s)
1	168	160	4.3 x 10^{-4}
2	151	152	3.5 x 10^{-4}
3	152	156	4.4 x 10^{-4}
5	162	156	3.7 x 10^{-4}

One very important parameter in reporting the diffusivity is the temperature. Heat-flow simulations were done to determine the average liquid temperature during the course of the experiment. For small temperature ranges, the temperature dependence of the diffusivity is expected to be linear. This view is supported by Stillinger-Weber calculations of the diffusivity temperature dependence[11,12]. As shown in Fig. 3, the average liquid temperature is very near T_m. In fact, the simulations indicate that the time-averaged temperature ranges from T_m+3 K at the surface to T_m+12 K near the full-melt depth. Therefore, the measured diffusivity should correspond to the average melt temperature, which in this case is T_m.

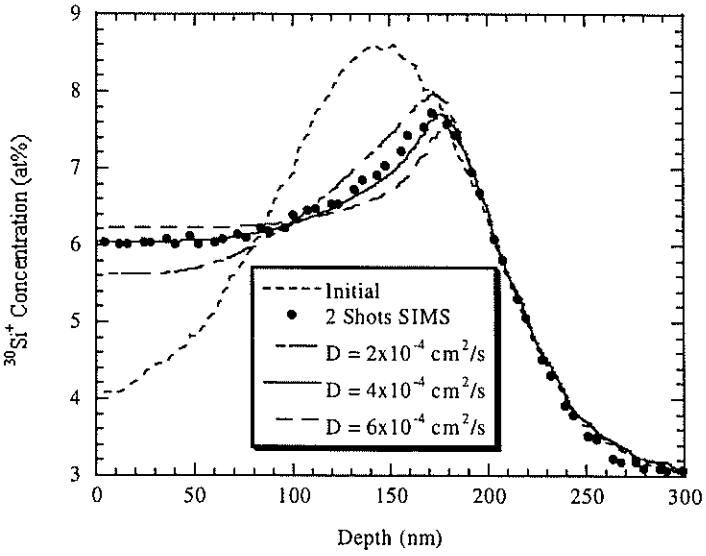

Fig. 2. Comparison between experimental SIMS concentration profile and simulated diffusion profiles after 2 laser shots with diffusivities of 2, 4, and 6 x 10^{-4} cm^2/s.

With certain restrictions, it can be shown that the effective liquid diffusivity is equal to the diffusivity at T_m. A flat liquid temperature distribution in z (resulting from, e.g., a virtually infinite liquid thermal conductivity) and a linear melting and freezing velocity response ($v \propto [T - T_m]$ where T is the crystal/melt interface temperature) can be shown to yield a temporal temperature profile at any depth (see Fig. 3) for which the integral of the portion of the curve above T_m is equal and opposite to that below T_m. This implies that the average liquid temperature is T_m at all depths. If the temperature dependence of the liquid diffusivity is linear, then the calculated diffusivity is a function of only the average temperature T_m. Any corrections to this model result from deviations from the above assumptions. The assumption most likely to be in error is the lack of a temperature gradient in the liquid during melt-in.

Convective contamination is always a concern in liquid diffusion measurements. Buoyancy-driven convection occurs as a result of temperature gradients within the specimen. Instabilities leading to natural convection[19] can occur if the Rayleigh number R > 1700. For the geometry of this experiment, $R = 6 \times 10^{-11}$. Since R has a cubic dependence on the thickness of the liquid layer, the likelihood of buoyancy-driven convection becomes significant only at melt depths > 5 mm, which is much greater than the 180 nm melt depths observed in this work.

Marangoni convection results from the temperature dependence of the surface tension and surface temperature gradients. Calculations of surface tension-driven convection using the Stokes solution to a suddenly accelerated flat plate in an infinite liquid[20] and the surface temperature variations identified in the heat-flow simulations indicate that diffusive transport is 2×10^{7} times faster than transport in z due to Marangoni convection. This results primarily from the negligible overheating of the liquid but also from the aspect ratio of the specimen, as the velocity of Marangoni-induced currents in z is reduced from the surface radial velocity by the depth-to-width ratio of the melt. Buoyancy- and surface tension-driven convection currents both tend to flow in the same direction, but the probability of either contributing to mass transport in this experiment is very low.

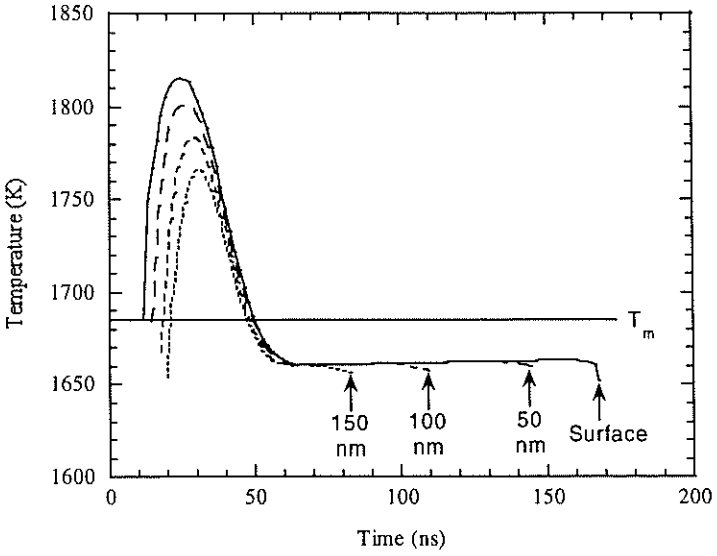

Fig. 3. Liquid temperature temporal profiles at various depths determined by heat-flow calculations. The surface (solid line) melts first and freezes last, while material at 150 nm depth (dotted curve) melts later and freezes sooner. When the solidification front passes a given depth, the local temperature suddenly drops from the essentially steady-state liquid and undercooled interface value of 1660 K during solidification (see features at 60 to 170 ns).

Summary

The silicon liquid self-diffusivity was determined by pulsed laser melting of $^{30}Si^{+}$ ion implanted silicon-on-insulator thin films. One-dimensional diffusion simulations were utilized to match the final $^{30}Si^{+}$ experimental concentration profile given the initial concentration profile and the melt profile. The silicon liquid self-diffusivity at the melting point is $(4.0 \pm 0.5) \times 10^{-4}$ cm^2/s. Calculations of Marangoni and buoyancy driven convection indicate that convective contamination is unlikely.

This research was sponsored by NASA grant NAG8-1256. The scientific insights and programming expertise of Michael O. Thompson of Cornell University are gratefully

acknowledged. The samples were prepared at the Cornell Nanofabrication Facility with the expert assistance of Michael Skvarla. Ion implantation was performed in the Surface Modification and Characterization Research Center at Oak Ridge National Laboratory. SIMS measurements were made by Thomas Mates in the Materials Department at the University of California at Santa Barbara. Howard Stone and Thomas Powers are acknowledged for valuable discussions on convection.

References

*corresponding author
[1]R. S. Sposili and J. S. Im, Appl. Phys. A **67,** 273 (1998).
[2]D. Toet, M. O. Thompson, P. M. Smith, and T. W. Sigmon, Appl. Phys. Let. **74**, 2170 (1999).
[3]T. Iida and R. I. L. Guthrie, *The Physical Properties of Liquid Metals* (Clarendon, Oxford, England, 1993) p. 199.
[4]L. B. Jalbert, F. Rosenberger, and R. M. Banish, J. Phys. Condens. Matter **10**, 7113 (1998).
[5]D. P. Brunco, M. O. Thompson, D. E. Hoglund, M. J. Aziz, and H.-J. Gossmann, J. Appl. Phys. **78**, 1575 (1995).
[6]J. R. Chelikowsky, N. Troullier, and N. Binggeli, Phys. Rev. B **49**, 114 (1994).
[7]I. Stich, R. Car, and M. Parrinello, Phys. Rev. B **44**, 4262 (1991).
[8]R. Virkkunen, K. Laasonen, and R. M. Nieminen, J. Phys. Condens. Matter **3**, 7455 (1991).
[9]C. Z. Wang, C. T. Chan, and K. M. Ho, Phys. Rev. B **45**, 12227 (1992).
[10]G. Servalli and L. Colombo, Europhys. Lett. **22**, 107 (1993).
[11]W. Yu, Z. Q. Wang, and D. Stroud, Phys. Rev. B **54**, 13946 (1996).
[12]K. Kakimoto, J. Appl. Phys. **77**, 4122 (1995).
[13]J. Q. Broughton and X. P. Li, Phys. Rev. B **35**, 9120 (1987).
[14]M. O. Thompson, G. J. Galvin, J. W. Mayer, P. S. Peercy, J. M. Poate, D. C. Jacobson, A. G. Cullis, and N. G. Chew, Phys. Rev. Lett. **52**, 2360 (1984).
[15]M. O. Thompson, Ph.D. thesis (Cornell University, Ithaca, New York, 1984).
[16]P. Baeri and S. U. Campisano, in *Laser Annealing of Semiconductors* (Academic Press, London, 1982) p. 75.
[17]M. J. Aziz, C. W. White, J. Narayan, and B. Stritzker, in *Energy Beam-Solid Interactions and Transient Thermal Processing* (Editions de Physique, Paris, 1985), p. 231.
[18]Solution of one-dimensional diffusion equation with moving interface by Crank-Nicholson algorithm, M. O. Thompson (1998).
[19]P. H. Roberts, "On Non-Linear Bérnard Convection," in *Non-Equilibrium Thermodynamics: Variational Techniques and Stability* (University of Chicago, Chicago, 1966) p. 126.
[20]J. P. Longtin, K. Hijikata, and K. Ogawa, Int. J. Heat Mass Trans. **42**, 85 (1999).